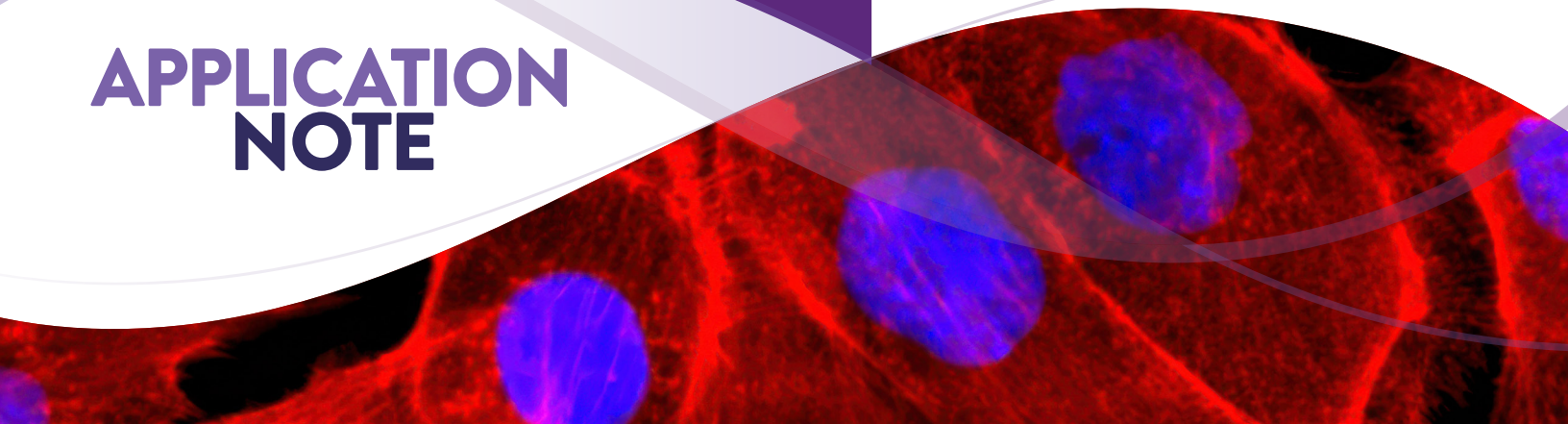# TRANSCRIPTOMIC PREDICTORS OF POLY (ADP-RIBOSE) POLYMERASE (PARP) INHIBITOR SENSITIVITY IN COLON CANCER CELL LINES

Ajeet P. Singh, PhD

ABSTRACT

Poly (ADP-ribose) polymerase (PARP) inhibitors have demonstrated therapeutic efficacy across several cancer types; however, their clinical utility in colon cancer remains unclear. To elucidate the molecular determinants of PARP inhibitor sensitivity in colon cancer cell lines, we used high-throughput RNA sequencing to analyze transcriptomic profiles. We identified distinct transcriptomic subtypes with differential sensitivity to PARP inhibition and discovered key pathways associated with drug response. These findings suggest that specific molecular signatures may underline variability in PARP inhibitor efficacy, providing novel insights into potential biomarkers for guiding patient stratification and future therapeutics.

INTRODUCTION

Colorectal cancer (CRC) remains one of the leading causes of cancer-related morbidity and mortality worldwide.[1] Despite advances in early detection and treatment, therapeutic resistance and disease recurrence continue to pose significant clinical challenges. Poly (ADP-ribose) polymerase (PARP) inhibitors, originally developed for treating tumors with homologous recombination deficiencies such as BRCA-mutated breast and ovarian cancers,[2,3] have shown promising therapeutic potential against CRC.[4] However, the response to PARP inhibition in CRC is heterogeneous, and the molecular determinants underlying this variability are not fully understood.[5]

Transcriptomic profiling offers a powerful approach to uncover gene expression patterns and signaling pathways that may predict therapeutic response. By analyzing the transcriptomic landscapes of colon cancer cell lines with varying sensitivity to PARP inhibitors, we can identify biomarkers and molecular signatures associated with drug efficacy. Such insights are critical for guiding patient stratification and optimizing the clinical application of PARP inhibitors in CRC.

In this study, we systematically investigated the relationship between transcriptomic signatures and PARP inhibitor response across a panel of colon cancer cell lines. Through integrative bioinformatic analyses, including differential gene expression, pathway enrichment, and predictive modeling, we elucidated the molecular features that correlate with sensitivity or resistance to PARP inhibition. Our findings contribute to a growing body of evidence supporting precision oncology approaches in CRC treatment.

MATERIALS AND METHODS

ACQUISITION AND CULTIVATION OF CRC CELL LINES

Colorectal cancer (CRC) cell lines Caco-2 (ATCC® HTB-37™), DLD-1 (ATCC® CCL-221™), HCT 116 (ATCC® CCL-247™), HT-29 (ATCC® HTB-38™), SW480 (ATCC® CCL-228™), were procured from the ATCC repository, ensuring the use of authenticated and well-characterized biological

materials. Each cell line was cultured under rigorously controlled laboratory conditions, with cultivation protocols tailored to the specific requirements of individual lines (Figure 1). All procedures adhered to ISO 9000 quality standards to maintain consistency and reproducibility across experiments. To account for biological variability and strengthen the reliability of downstream molecular analyses, five independent biological replicates were generated for each cell line. Detailed records of culture conditions—including media composition, incubation parameters, and passage numbers—were maintained to ensure traceability and reproducibility. Cells were harvested during the logarithmic growth phase, typically at 70–80% confluency, to capture optimal cellular activity. Following harvest, cells were pelleted by centrifugation at 150–450 × g, depending on cell type and density, in preparation for nucleic acid extraction.

CELL CULTURE
Authenticated cell lines cultured under controlled conditions

NUCLEIC ACID EXTRACTION
Total RNA & genomic DNA extracted from five biological replicates

BIOINFORMATICS ANALYSIS
Quality control, alignment, quantification, and variant calling

Strict quality acceptance criteria at each step

RNAseq and WES on Illumina platforms

Quality control, alignment, quantification, and variant calling

Final curated datasets deposited into the QIAGEN Digital Insights OmicSoft ATCC Cell Line Land database

Figure 1: **Overview of the ATCC sequencing & bioinformatics workflow.** The molecular profiling pipeline for human cell lines collections consists of four standardized steps: (1) Cell culture of authenticated lines under controlled conditions, (2) extraction of total RNA and genomic DNA from five independent biological replicates, (3) next-generation sequencing using RNAseq and whole-exome sequencing (WES) on Illumina platforms, and (4) bioinformatics analysis including quality control, alignment, quantification, and variant calling. Final curated datasets are deposited into the QIAGEN Digital Insights OmicSoft ATCC Cell Line Land database.

NUCLEIC ACID EXTRACTION

Total RNA was extracted from each biological replicate using the QIAcube automated system with the RNeasy Mini QIAcube Kit (QIAGEN). Frozen samples were thawed and prepared for RNA extraction according to ATCC's work instructions. Extracted samples were tested for RNA purity and RNA quality using the Thermo Fisher Scientific Nanodrop (A260/A280 1.8 ≥ x ≤ 2.2) and Agilent Tapestation (≥ 6.5), respectively.

NEXT-GENERATION SEQUENCING

Automated RNA-seq NGS library preparation was performed on the Eppendorf epMotion 5075 Liquid Handler using the Illumina Stranded mRNA Prep, Ligation kit. Prepared NGS libraries were assessed by quantitative analysis using the Invitrogen Qubit dsDNA High Sensitivity Assay Kit and qualitative analysis using the Agilent 4200 TapeStation and D5000 ScreenTape System. Libraries were loaded on an Illumina P3 200-cycle Reagent Kit and sequenced on the NextSeq 2000 platform.

ROBUST BIOINFORMATICS ANALYSIS AND DATA CURATION

Raw sequencing reads were corrected for broken read pairs as needed with bbmap's repair.sh (<5% of samples) and trimmed with fastp to remove any lingering adapter sequences or extraneous poly-g tails. Trimmed reads were then mapped to the RefSeq human genome reference GRCh38.p14 with the STAR mapping software utilizing its options for 2-pass mapping for sensitive novel junction discovery. The output logs from STAR were used to ensure ≥ 18M input reads and ≥ 70% uniquely mapped reads via a custom R script.

DATA INTEGRATION INTO QIAGEN OMICSOFT ATCC CELL LINE LAND

Final curated datasets are deposited into the QIAGEN Digital Insights OmicSoft ATCC Cell Line Land Bioinformatics Software (https://digitalinsights.qiagen.com/atcc-cell-line-land/). This centralized, searchable resource provides researchers with access to high-quality molecular profiles of human and mouse cell lines. Users can explore gene expression patterns, variant landscapes, and other molecular features to support biological discovery, drug development, and translational research. The database is continuously updated and maintained to reflect the latest data and analytical improvements. The QIAGEN Ingenuity Pathway Analysis (IPA) of the differentially expressed genes was performed for biological pathways and gene network discovery.

## EXPLORATION OF FUNCTIONAL GENOMIC DATA USING UCSC XENA BROWSER

We used the UCSC Xena Functional Genomics Explorer (https://xena.ucsc.edu) to interactively analyze and visualize large-scale genomic datasets. This platform allows seamless integration of publicly available and user-uploaded data, enabling exploration of relationships between genomic features—such as mutations and gene expression—and phenotypic traits. Using the Xena Browser's intuitive interface, we performed correlation analyses and visualized results through built-in statistical tools.

RESULTS

EXPRESSION PATTERNS OF COMMON CANCER GENES IN CULTURED COLON CANCER CELL LINES

The expression profiles of oncogenes and tumor suppressor genes play a critical role in shaping tumor behavior and therapeutic response, particularly in the context of DNA repair deficiencies targeted by PARP inhibitors. Well-established oncogenes (e.g., *ABL1*, *KRAS*, *PIK3CA*, *EGFR*, and *MYC*) and tumor suppressors (e.g., *BRCA1*, *TP53*, *PTEN*, **RB1**, and *CDKN2A*) are frequently mutated or aberrantly expressed in colon cancer. To explore the expression profiles of these genes in our panel of colon cancer cell lines, we utilized QIAGEN Digital Insights OmicSoft ATCC Cell Line Land to generate a heatmap of mRNA expression patterns (Figure 2).

Our analysis revealed that HCT 116, HT-29, and SW480 cell lines exhibit elevated expression of *KRAS*, *PIK3CA*, *EGFR*, *MYC*, *BRCA1*, *TP53*, *RB1*, and *CKN2A*. In contrast, Caco-2 cells, which are capable of differentiating into a phenotype resembling small intestinal enterocytes when cultured under specific conditions, showed enrichment of *ABL1*, *KRAS*, and *BRCA1* and attenuation of *PIK3CA*, *EGFR*, *MYC*, *TP53*, *PTEN*, *RB1*, and *CDKN2A*. Similarly, DLD-1 cells expressed *PIK3CA*, *EGFR*, *BRCA1*, *PTEN*, and *RB1*, but had reduced levels of *ABL1*, *KRAS*, *MYC*, *TP53*, and *CDKN2A*. Notably, HCT 116 cells overexpressed all analyzed genes (Figure 2). HT-29 cells also expressed all genes, albeit with reduced levels of *ABL1*, *EGFR*, and *BRCA1*. SW480 displayed a similar expression pattern to HCT 116, except for diminished expression of *BRCA1* and *PTEN*. These findings underscore the molecular heterogeneity among these colorectal cancer cell lines and suggest differential responses to PARP inhibitor treatment, consistent with previous studies.[5]
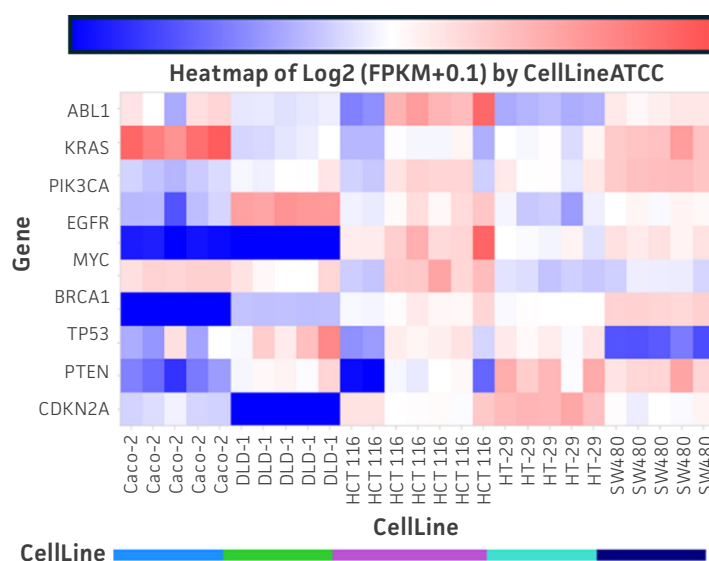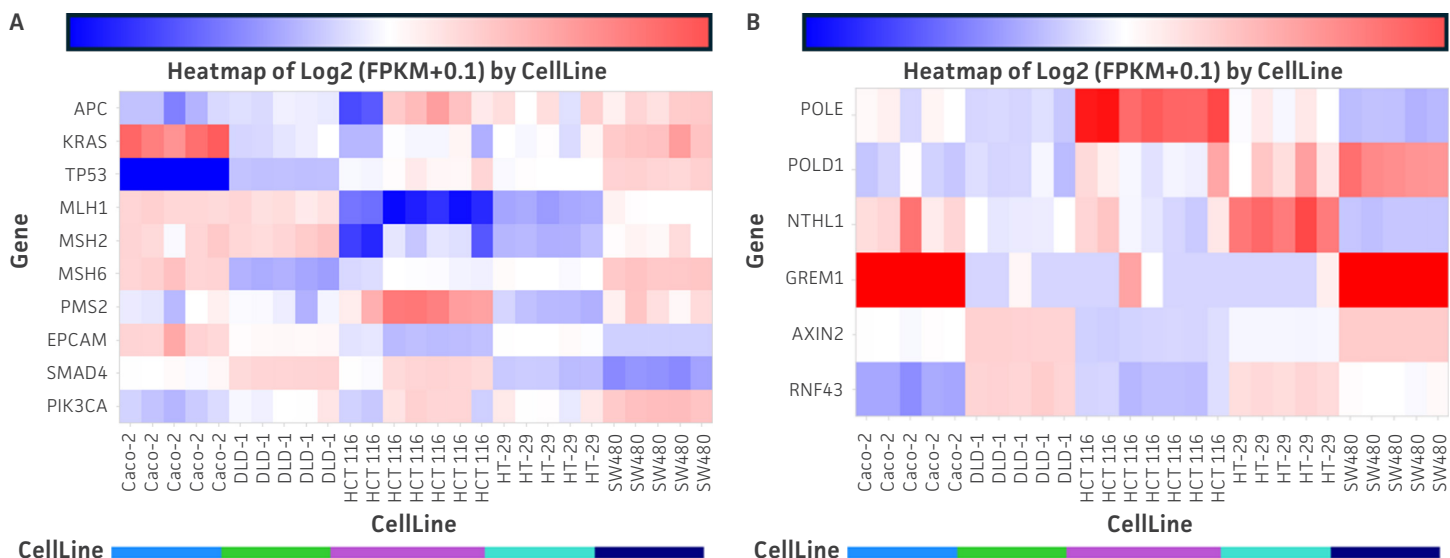

Figure 2: Heatmap of oncogene and tumor suppressor gene expression across colon cancer cell lines. The heatmap displays log2-transformed FPKM values (log2[FPKM + 0.1]) for key oncogenes and tumor suppressor genes across five colon cancer cell lines: Caco-2, DLD-1, HCT 116, HT-29, and SW480. Cell lines were analyzed in quintuplicate—except HCT 116, which was included in septuplicate—to ensure data reproducibility and scientific rigor. Expression levels are color-coded with blue indicating lower expression and red indicating higher expression. Data visualization was performed using ATCC Cell Line Land.

DIFFERENTIAL EXPRESSION OF DNA REPAIR AND TUMORIGENESIS-ASSOCIATED GENES IN COLON CANCER CELL LINES

Next, we examined the expression patterns of key genes frequently implicated in colon cancer, particularly those involved in DNA mismatch repair (MMR) and tumorigenic signaling pathways. The MMR genes—*MLH1*, *MSH2*, *MSH6*, and *PMS2*—showed differential expression across the analyzed cell lines (Figure 3A), suggesting potential dysregulation of the MMR pathway, a hallmark of microsatellite instability and Lynch syndrome.[6–8]

Additionally, genes involved in cell proliferation and signaling—*APC*, *EPCAM*, *SMAD4*, and *PIK3CA*—were aberrantly expressed, consistent with their established roles in colorectal tumorigenesis (Figure 3A).[6–8] A broader panel of colon cancer-associated genes was also assessed, and their mRNA expression profiles were visualized using a heatmap (Figure 3B). Among these, *GREM1* was notably overexpressed in Caco-2 and SW480 cells, while *POLE*, *POLD1*, and *NTHL1* exhibited elevated expression in HCT 116, SW480, and HT-29 cells, respectively. These findings highlight the molecular heterogeneity across colon cancer cell lines and underscore the importance of selecting appropriate models for functional studies.
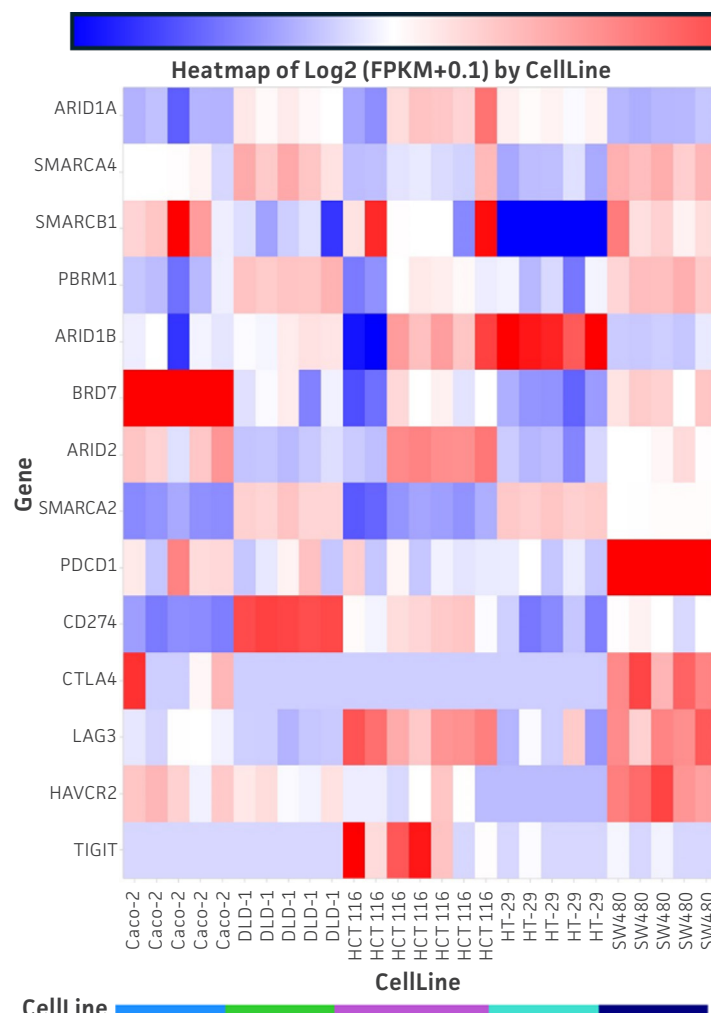
Figure 3: Heatmap of gene expression in colon cancer cell lines. The heatmap displays log2-transformed FPKM values (log2[FPKM + 0.1]) for key colon cancer-associated genes across five colon cancer cell lines: Caco-2, DLD-1, HCT 116, HT-29, and SW480. (A) Frequently mutated genes analyzed in each cell line are represented across multiple replicates (Caco-2 and DLD-1, HT-29, and SW480 in quintuplicate and HCT 116 in septuplicate). Expression levels are color-coded, with blue indicating lower expression and red indicating higher expression. (B) Heatmap of rarely associated gene expression for additional colon cancer-associated genes across five colon cancer cell lines. Cell line identities are represented by color-coded bars at the bottom: blue (Caco-2), green (DLD-1), purple (HCT 116), cyan (HT-29), and dark blue (SW480).

EXPRESSION PROFILES OF CHROMATIN REMODELING AND IMMUNE CHECKPOINT GENES IN COLON CANCER CELL LINES

To further characterize the molecular landscape of colon cancer cell lines, we analyzed the expression profiles of genes involved in chromatin remodeling and immune checkpoint regulation (Figure 4), both of which play critical roles in tumor progression and therapeutic response. Chromatin remodeling factors regulate chromatin accessibility, DNA repair, and transcriptional control.[9] Mutations or altered expressions in SWI/SNF components are frequently observed in colorectal and other cancers, contributing to tumorigenesis, immune evasion, and resistance to therapy.[10,11] A heatmap of log2-transformed FPKM values (log2[FPKM + 0.1]) revealed distinct expression patterns of the genes across the Caco-2, DLD-1, HCT 116, HT-29, and SW480 cell lines. Genes encoding components of the SWI/SNF chromatin remodeling complex—*ARID1A*, *SMARCA4*, *SMARCB1*, *PBRM1*, *ARID1B*, *BRD7*, *ARID2*, and *SMARCA2*—exhibited variable expression levels, suggesting differential epigenetic regulation among the cell lines. Notably, *ARID1A* and *SMARCA4* were moderately to highly expressed across most lines, while *SMARCB1* and *PBRM1* showed reduced expression in DLD-1 and HT-29. In contrast, *ARID2* and *SMARCA2* were more prominently expressed in HCT 116 and HT-29, respectively (Figure 4). These patterns suggest differential epigenetic regulation and potential vulnerabilities that could be exploited therapeutically.

Evaluation of the immune checkpoint genes *PDCD1 (PD-1), CD274 (PD-L1), CTLA4, LAG3, HAVCR2 (TIM-3)*, and *TIGIT* revealed low to moderate levels of gene expression, with CD274 showing relatively higher expression in DLD-1, SW480, and HCT 116. *PDCD1* and *CTLA4* were minimally expressed across all cell lines except SW480 (Figure 4), consistent with their predominant expression in immune cells rather than tumor cells.[12,13] These findings underscore the heterogeneity of both chromatin remodeling and immune regulatory gene expression in colon cancer models and highlight their relevance in guiding preclinical model selection and therapeutic targeting strategies.

Figure 4: **Expression heatmap of chromatin remodeling and immune checkpoint genes in colon cancer cell lines.** Log2(FPKM + 0.1) values are shown for selected genes across the Caco-2, DLD-1, HCT 116, HT-29, and SW480 cell lines. Red indicates high expression; blue indicates low expression. Multiple replicates were used to ensure reproducibility and scientific rigor.

## PATHWAY ENRICHMENT ANALYSIS REVEALS DYSREGULATION OF RIBOSOMAL BIOGENESIS, TRANSCRIPTION, AND STRESS RESPONSES

Ingenuity pathway analysis (IPA) identified multiple significantly enriched pathways in colon carcinoma cell lines, reflecting widespread transcriptional and metabolic reprogramming. The rRNA processing pathway demonstrated the highest level of enrichment (−log(p-value) = 14.1; z-score = 6.564), indicative of enhanced ribosomal biogenesis. Similarly, the generic transcription pathway (z-score = 6.277) and RHO GTPase Cycle (z-score = 1.86) were activated, suggesting upregulation of global transcriptional activity and cytoskeletal signaling, respectively.

Notably, IL–10 signaling was enriched but exhibited a negative z-score (−0.707), suggesting suppression of anti-inflammatory signaling. In contrast, ID1 signaling (z-score = 1.947) (Figure 5) and nonsense-mediated decay (z-score = 4.707) were positively regulated, consistent with increased transcriptional repression and mRNA surveillance activity.

Activation of the GCN2-mediated amino acid deficiency response (z-score = 4.899) points to nutrient stress signaling, while SREBF-mediated lipid biosynthesis was suppressed (z-score = −2.324), indicating downregulation of lipid metabolic pathways. The CLEAR pathway, associated with lysosomal biogenesis and autophagy, showed minimal activation (z-score = 0.302), suggesting modest lysosomal modulation.
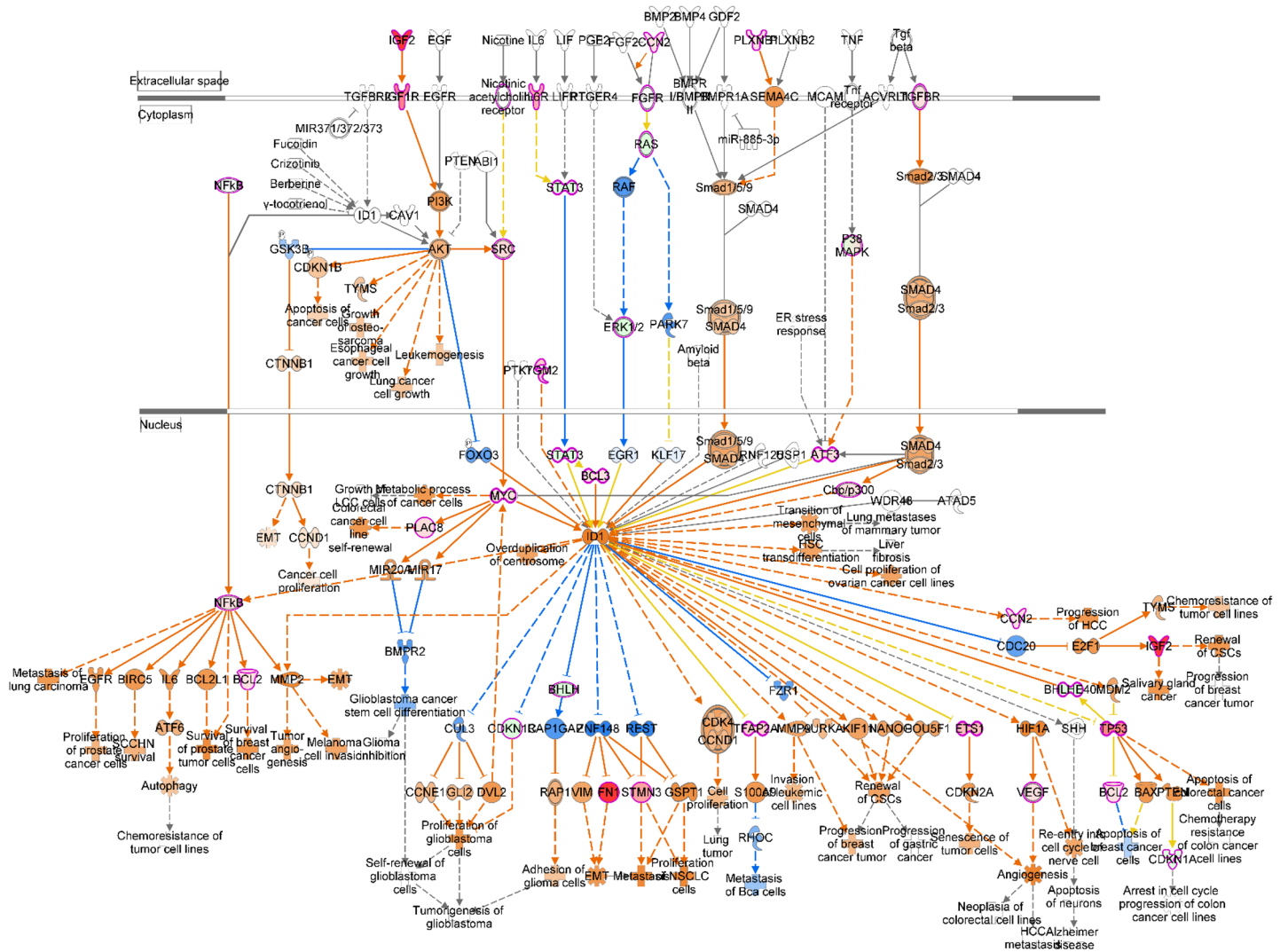
Figure 5: Ingenuity Pathway Analysis of the ID1 Signaling Pathway. The ID1 pathway illustrates the predicted activation state and molecular interactions within the ID1 signaling pathway based on differential gene expression data. ID1, a helix-loop-helix transcriptional regulator, is implicated in cell proliferation, differentiation, and tumor progression. Upstream and downstream components are color-coded based on expression changes and predicted activation states. The pathway was significantly enriched (−log(p-value) = 7.47) with a moderate activation z-score of 1.947, suggesting upregulation of ID1-associated signaling. Molecules with increased expression are shown in red, decreased expression in green, and predicted activation states are indicated by orange (activated) or blue (inhibited) outlines.

UPSTREAM REGULATOR ANALYSIS HIGHLIGHTS ESTROGENIC AND ONCOGENIC DRIVERS
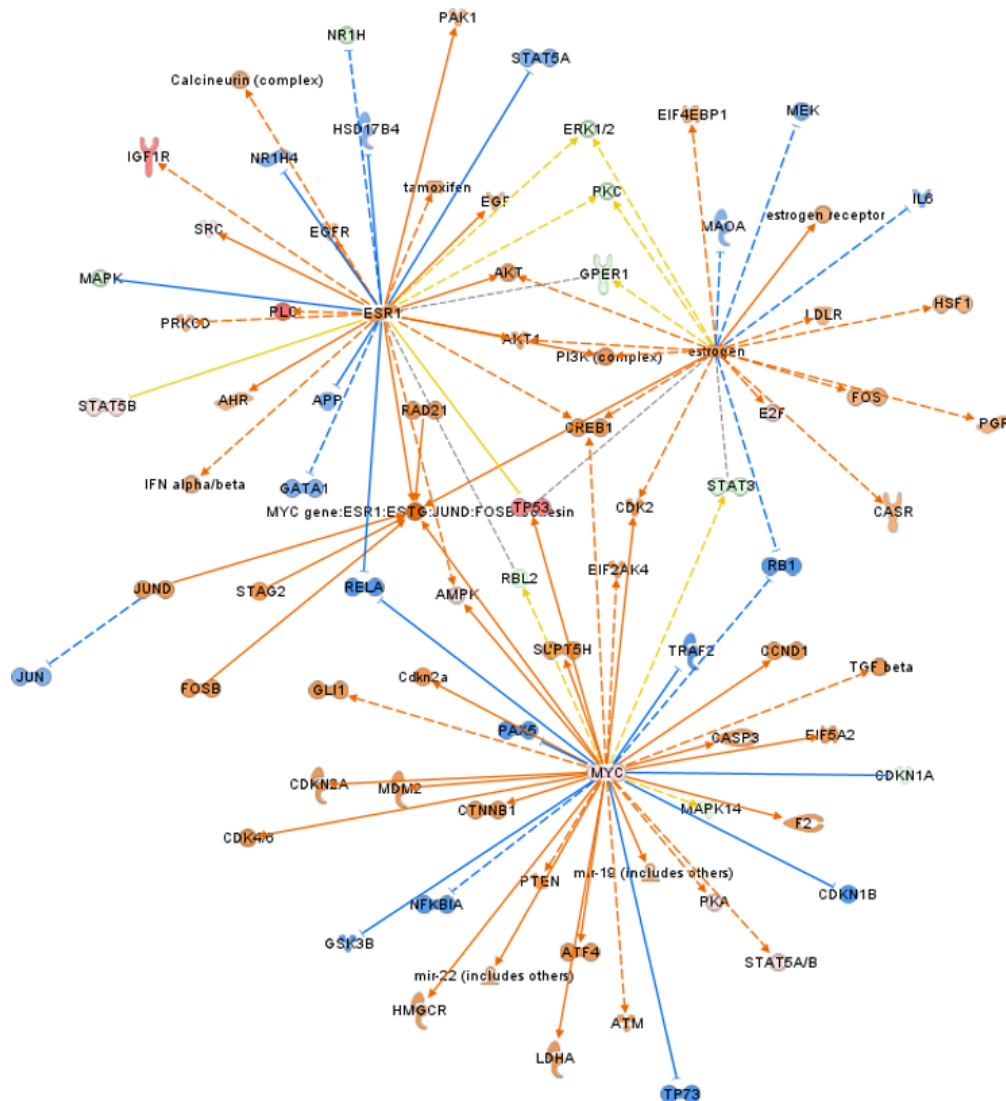
Upstream regulator analysis via IPA identified several transcriptional regulators with significant enrichment and predicted activity states (Figure 6A). Beta-estradiol emerged as the most significantly enriched upstream regulator (p = 1.78 × 10^{-26}), with a high activation z-score (3.876), indicating a strong estrogenic influence on gene expression. MYC, a well-established oncogenic transcription factor, was also predicted to be activated (fold change = 2.666; z-score = 3.745), consistent with its role in promoting proliferation and metabolic reprogramming.

GLI1, a key effector of Hedgehog signaling, was significantly inhibited (z-score = −2.299), suggesting pathway suppression. HNF4A and KRAS were identified with strong statistical support (p < 1.3 × 10^{-18}), although no definitive activation state was predicted. Dexamethasone, a synthetic glucocorticoid, exhibited a negative expression trend (fold change = −0.8), potentially reflecting anti-inflammatory signaling.

Additional regulators of interest included TP53 (fold change = 23.035), ESR1, and the CG complex, all of which demonstrated significant enrichment, underscoring their potential involvement in the transcriptional landscape of colon carcinoma cells.

A

Upstream Regulator	Predicted Activation State	Activation z-score	p-value of overlap
Beta-estradiol	Activated	3.876	1.78E-26
HNF4A		-0.918	1.07E-19
KRAS		1.697	1.24E-18
Dexamethasone		-0.8	6.82E-17
MYC	Activated	3.745	1.67E-16
CG (complex)		-0.202	1.95E-16
GLI1	Inhibited	-2.299	6.9E-16
TP53		0.137	3.3E-15
ESR1		1.488	6.88E-15

B

Figure 6: Upstream regulators and causal network of oncogenic regulators. (A) Upstream regulator analysis identified several key molecules with significant predicted activity based on gene expression patterns. Beta-estradiol and MYC were strongly predicted to be activated (z-scores: 3.876 and 3.745, respectively; p-values: 1.78×10^{-26} and 1.67×10^{-16}) while GLI1 was inhibited (z-score: -2.299; p-value: 6.9×10^{-16}). Other regulators such as KRAS and ESR1 showed moderate activation (z-scores: 1.697 and 1.488) whereas HNF4A and dexamethasone exhibited slight inhibition. TP53 and CG (complex) had minimal z-scores, indicating uncertain activation states despite statistically significant overlaps. (B) The network illustrates predicted upstream regulators influencing transcriptional programs relevant to tumorigenesis. Central hubs include MYC and ESR1, which integrate signals from upstream effectors such as STAT3, ERBB2, and IFN alpha/beta receptor. Nodes represent genes or proteins, while edges denote directional regulatory relationships, color-coded by interaction type (activation, inhibition, or context-dependent). This system-level view highlights potential regulatory bottlenecks and therapeutic targets in oncogenic signaling pathways.

UPSTREAM CAUSAL NETWORK ANALYSIS

To elucidate the regulatory architecture underlying oncogenic signaling in our dataset, we observed an upstream causal network centered on transcriptional regulators with established roles in tumorigenesis. The resulting network revealed two major hubs—MYC and ESR1—that integrate signals from a diverse array of upstream effectors, including STAT3, ERBB2, and IFN alpha/beta receptor (Figure 6B). These nodes are known to participate in pathways governing cell proliferation, immune modulation, and endocrine signaling, all of which are critical in cancer progression.

Edges within the network are directionally annotated and color-coded to reflect the nature of the regulatory influence (activation, inhibition, or context-dependent modulation). This structure highlights potential master regulators and signaling bottlenecks. Notably, the convergence of interferon signaling with ERBB2 and MYC pathways suggests a mechanistic link between immune response and proliferative signaling, which may inform therapeutic strategies targeting immune-oncology interfaces.

This network-based approach provides a system-level perspective on how upstream molecular cues orchestrate oncogenic transcriptional programs, offering insights into candidate biomarkers and potential intervention points for precision oncology.

DIFFERENTIAL GENE EXPRESSION OF DNA REPAIR AND IMMUNE CHECKPOINT GENES PREDICTS OVERALL SURVIVAL

We used the UCSC Xena functional genomics dataset to investigate whether genes that show differential expression in colon cancer cell lines are associated with patient survival outcomes. Kaplan-Meier survival analysis with UCSC Xena functional genomics explorer revealed a statistically significant difference in overall survival between patients with high and low *GREM1* expression levels. Overexpression of *GREM1* is observed in various cancers (e.g., colorectal, breast, glioblastoma), where it contributes to cancer stem cell (CSC) maintenance, immune evasion, and tumor progression by inhibiting BMP-mediated differentiation.[14] It also interacts with Wnt/Frizzled and FGF→SHH pathways, further influencing CSC stemness and tumorigenesis. Patients with *GREM1* expression ≥10.54 (red line, n = 163) exhibited reduced survival probability compared to those with expression <10.54 (blue line, n = 163). The log-rank test yielded a p-value of 0.01578 and a test statistic of 5.828, indicating that elevated *GREM1* expression is associated with poorer prognosis (Figure 7). The survival curves begin to diverge early and continue to separate over time, suggesting a consistent impact of *GREM1* expression on patient outcomes.

Conversely, high *CTLA4* expression (red line) was associated with significantly increased survival (p = 0.05562) (Figure 7), highlighting its potential role in immune modulation and prognosis. In contrast, for both *POLD1* and *POLE*, the survival curves for high and low expression groups did not show a statistically significant difference over the follow-up period of approximately 4,000 days (Figure 7). The log-rank test yielded p-values of 0.6025 and 0.4072, and test statistics of 0.2713 and 0.6870, respectively, indicating that the expression levels of *POLE* and *POLD1* were not significantly associated with overall survival in this cohort. The number of patients at risk declined similarly in both groups over time. These results highlight the importance of *GREM1* and *CTLA4* as potential predictors of cancer survival, reflecting their roles in DNA repair and immune regulation. In contrast, *POLE* and *POLD1* showed limited value as prognostic markers in this dataset.[14]
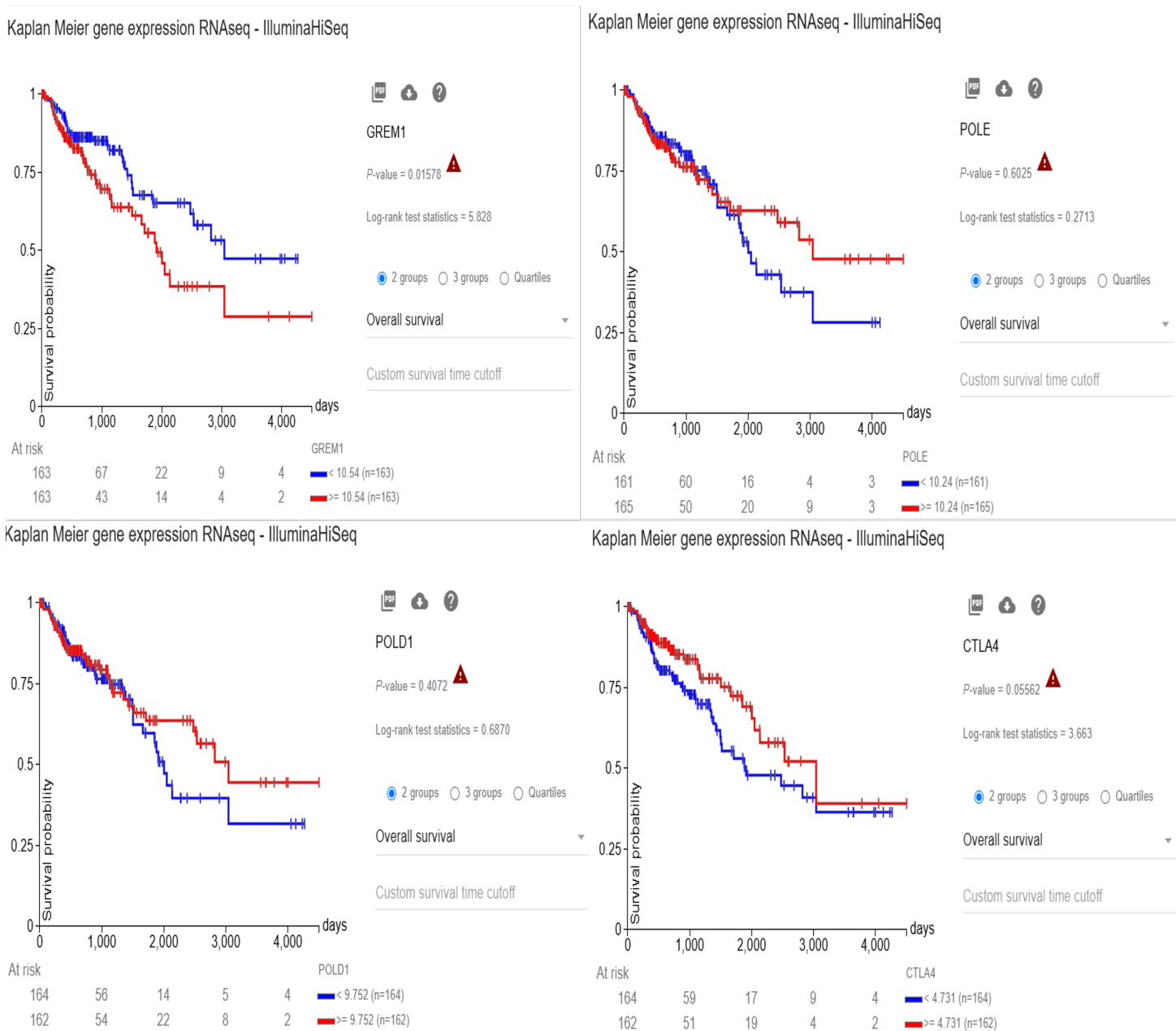
Figure 7: Kaplan-Meier survival analysis of patients stratified by gene expression levels (GREM1, POLE, POLD1, and CTLA4) using RNA sequencing data (Illumina HiSeq platform). Patients were divided into two groups based on gene expression: low expression (blue line) and high expression (red line). Survival probability over time (in days) was significantly associated with *GREM1* and *CTLA4* expression. Specifically, high *GREM1* expression and low *CTLA4* expression were associated with poorer overall survival. In contrast, no significant survival differences were observed between expression groups for *POLE* and *POLD1*.

DISCUSSION AND CONCLUSION

In this study, we conducted a detailed transcriptomic analysis of colon cancer cell lines to better understand what drives their sensitivity to PARP inhibitors. By combining gene expression profiling, pathway enrichment, and survival analysis, we uncovered distinct molecular signatures and regulatory networks that appear to influence how these cells respond to treatment.

Our results show that colon cancer cell lines vary widely in the expression of key oncogenes, tumor suppressors, DNA repair genes, and immune checkpoint regulators. For instance, some cell lines showed high levels of *BRCA1*, suggesting they may be proficient in homologous recombination—a factor that could affect how well they respond to PARP inhibition. On the other hand, reduced expression of mismatch repair genes in certain cell lines points to alternative DNA repair deficiencies that might make them more vulnerable to these drugs.

Pathway analysis revealed that processes like ribosomal biogenesis, transcriptional regulation, and stress responses are more active in sensitive cell lines, hinting at a role for metabolic and transcriptional reprogramming in shaping drug response. We also observed

suppression of lipid biosynthesis and IL-10 signaling, highlighting the complex interactions between metabolism and immune signaling in determining treatment outcomes.

Our upstream regulator analysis identified MYC and ESR1 as key players in the transcriptional networks of these cells. Interestingly, we also saw a convergence of interferon signaling with ERBB2 and MYC pathways, suggesting a potential link between immune modulation and cell proliferation—an insight that could inform future combination therapies.

Survival analysis added another layer of insight: high GREM1 expression was linked to worse outcomes, while higher CTLA4 levels were associated with better survival. GREM1, a BMP antagonist, has been implicated in promoting cancer stem cell maintenance, immune evasion, and tumor progression. Its overexpression may contribute to genomic instability, a hallmark of tumors that are often sensitive to DNA damage response (DDR)-targeting therapies such as PARP inhibitors. PARP inhibitors exploit defects in homologous recombination repair to induce synthetic lethality, particularly in tumors with compromised DNA repair capacity. The association between GREM1 and poor survival may reflect an underlying vulnerability to such therapies, positioning GREM1 as a potential biomarker for PARP inhibitor responsiveness. Conversely, CTLA4 is a well-established immune checkpoint molecule that modulates T-cell activation. Its positive correlation with survival aligns with the therapeutic success of immune checkpoint inhibitors (ICIs), which have transformed treatment paradigms across multiple cancer types. Emerging evidence suggests that PARP inhibition can enhance tumor immunogenicity by increasing DNA damage and activating innate immune signaling, thereby improving the efficacy of ICIs. The observed survival benefit associated with CTLA4 expression supports this synergy and highlights the potential of combination therapies involving PARP inhibitors and immune checkpoint blockade. These findings underscore the potential of DNA repair and immune checkpoint genes as prognostic markers and tools for patient stratification.

In summary, our work sheds light on the transcriptomic features that may predict how colon cancer cells respond to PARP inhibitors. The gene signatures and pathways we identified could serve as valuable biomarkers and guide more personalized treatment strategies. Moving forward, these findings should be validated in clinical samples, and the potential for combining PARP inhibitors with other targeted therapies should be explored.

REFERENCES

1. Rawla P, Sunkara T, Barsouk A. Epidemiology of colorectal cancer: incidence, mortality, survival, and risk factors. Gastroenterol Rev 14: 89–103, 2019.
2. Mani C, et al. GLI1-targeting drugs induce replication stress and homologous recombination deficiency and synergize with PARP-targeted therapies in triple negative breast cancer cells. Biochim Biophys Acta BBA - Mol Basis Dis 1868: 166300, 2022.
3. Mittica G, et al. PARP Inhibitors in Ovarian Cancer. Recent Patents Anticancer Drug Discov 13: 392–410, 2018.
4. Bondar D, Karpichev Y. Poly(ADP-Ribose) Polymerase (PARP) Inhibitors for Cancer Therapy: Advances, Challenges, and Future Directions. Biomolecules 14: 1269, 2024.
5. Smeby J, et al. Molecular correlates of sensitivity to PARP inhibition beyond homologous recombination deficiency in pre-clinical models of colorectal cancer point to wild-type TP53 activity. eBioMedicine 59: 102923, 2020.
6. Riedinger CJ, et al. Characterization of mismatch-repair/microsatellite instability-discordant endometrial cancers. Cancer 130: 385–399, 2024.
7. Benusiglio PR, et al. Mismatch Repair Deficiency and Lynch Syndrome Among Adult Patients With Glioma. JCO Precis Oncol 7: e2200525, 2023.
8. Salem ME, et al. Relationship between MLH1 , PMS2 , MSH2 and MSH6 gene-specific alterations and tumor mutational burden in 1057 microsatellite instability-high solid tumors. Int J Cancer 147: 2948–2956, 2020.
9. Singh AP, Archer TK. Analysis of the SWI/SNF chromatin-remodeling complex during early heart development and BAF250a repression cardiac gene transcription during P19 cell differentiation. Nucleic Acids Res 42: 2958–2975, 2014.
10. Hao F, Zhang Y, Hou J, Zhao B. Chromatin remodeling and cancer: the critical influence of the SWI/SNF complex. Epigenetics Chromatin 18: 22, 2025.
11. Krishnamurthy N, et al. Chromatin remodeling (SWI/SNF) complexes, cancer, and response to immunotherapy. J Immunother Cancer 10(9): e004669, 2022.
12. Hao F, Zhang Y, Hou J, Zhao B. Chromatin remodeling and cancer: the critical influence of the SWI/SNF complex. Epigenetics Chromatin 18: 22, 2025.
13. Bakr A, et al. ARID1A regulates DNA repair through chromatin organization and its deficiency triggers DNA damage-mediated anti-tumor immune response. Nucleic Acids Res 52: 5698–5719, 2024.
14. Gao Y, De S, Brazil D P. The Role of GREMLIN1, a Bone Morphogenetic Protein Antagonist, in Cancer Stem Cell Regulation. Cells 14: 578, 2025.

DATA AVAILABILITY STATEMENT

All sequencing data generated and analyzed during this study are available through the QIAGEN Digital Insights OmicSoft ATCC Cell Line Land database (https://www.qiagen.com/us/products/discovery-and-translational-research/qiagen-omicsoft/). Access to the database may require a subscription or institutional license. Additional metadata and quality control metrics are available from the corresponding author upon reasonable request.

10801 University Boulevard
Manassas, Virginia 20110-2209

703.365.2700

703.365.2701

sales@atcc.org

www.atcc.org